
Principal components of piezo-optic tensor for $\text{Pb}_5\text{Ge}_3\text{O}_{11}$ crystals

¹Mytsyk B., ¹Demyanyshyn N., ²Adamenko D., ³Trubitsyn M. and ²Vlokh R.

¹Karpenko Physico-Mechanical Institute, 5 Naukova Street, 79601 Lviv, Ukraine

²Vlokh Institute of Physical Optics, 23 Dragomanov Street, 79005 Lviv, Ukraine

³Oles Honchar Dnipro National University, 49010 Dnipro, 72 Gagarin Avenue, Ukraine

Received: 12.05.2019

Abstract. Using an interferometric technique and a half-wave stress method, we determine experimentally the principal components π_{11} , π_{12} , π_{13} , π_{31} and π_{33} of the piezo-optic tensor π_{im} for lead germanate crystals. Following from the above data, elasto-optic coefficients p_{im} are calculated. The coefficient of acousto-optic (AO) figure of merit M_2 is estimated for the case of AO interactions with longitudinal acoustic waves. It is shown that, issuing from its maximal M_2 parameter ($M_2 = 24.3 \times 10^{-15} \text{ s}^3/\text{kg}$), $\text{Pb}_5\text{Ge}_3\text{O}_{11}$ can be compared to beta-barium borate or lead molybdate crystals. Moreover, this parameter exceeds essentially the values known for such notorious AO materials as, e.g., lithium niobate, crystalline quartz and fused silica.

Keywords: piezo-optic effect, interferometric methods, $\text{Pb}_5\text{Ge}_3\text{O}_{11}$ crystals.

UDC: 535.551

1. Introduction

Lead germanate $\text{Pb}_5\text{Ge}_3\text{O}_{11}$ belongs to the point group of symmetry 3 under normal conditions [1]. This trigonal-pyramidal group is characterized by a very complicated form of its piezo-optic tensor that contains 30 nonzero components, 12 of which are independent (11 invariant) [2]. In what the number of nonzero and/or independent piezo-optic components is concerned, the point symmetry group 3 is similar to the monoclinic groups, for which the piezo-optic tensor contains 20 nonzero components and 19 invariant ones. One can state that, from the viewpoint of piezo-optic effect, the point group 3 is indeed close to the low-symmetry groups, despite the fact that the crystals belonging to the group 3 are optically uniaxial. Similar situation is also peculiar for the rhombohedral symmetry group $\bar{3}$. This concerns all the other properties of the groups 3 and $\bar{3}$ described by the tensors of ranks higher than two.

As a consequence, experimental determination of all components of the piezo-optic tensor for the crystals belonging to the groups 3 and $\bar{3}$ is not a simple problem. In the present work, we begin to solve this problem for the first time. The main challenge here concerns determination of so-called non-principal and non-diagonal components of the piezo-optic matrix. We remind that the principal components are given by π_{ij} with $i, j = 1, 2$ and 3, while the diagonal ones, π_{ij} , are characterized by $i = j = 1, \dots, 6$. The main difficulties that appear when determining the non-principal and non-diagonal components of the piezo-optic tensor have earlier been thoroughly formulated and experimentally solved on the example of monoclinic triglycine sulfate $((\text{NH}_2\text{CH}_2\text{COOH})_3 \times \text{H}_2\text{SO}_4)$ [3] and tetragonal-dipyramidal calcium tungstate (CaWO_4) [4].

In the present work we start our studies of the piezo-optic coefficients (POCs) for the $\text{Pb}_5\text{Ge}_3\text{O}_{11}$ crystals from experimental determination of their principal POCs, i.e. the matrix

components π_{11} , π_{12} , π_{13} , π_{31} and π_{33} . Moreover, below we calculate the appropriate elasto-optic coefficients and estimate acousto-optic (AO) figure of merit that corresponds to the largest elasto-optic coefficients for lead germanate.

2. Experimental methods

$\text{Pb}_5\text{Ge}_3\text{O}_{11}$ crystals have been grown at the Oles Honchar Dnipro National University (Ukraine), using a known Czochralski method. Our crystals have the shape of a hexagonal prism, with the height ~ 3.5 cm and the cross section $\sim 2 \times 1$ cm².

To study the principal POCs, we have prepared samples of so-called direct cuts. These have two faces perpendicular to crystallographic axes c and a and one face parallel to ac plane. The samples have a cubic shape, with the sizes $\sim 6 \times 6 \times 6$ mm³. The Cartesian crystal-physical coordinate system XYZ has been chosen according to the rules $Z \parallel c$, $X \parallel a$ and $Y \perp ac$. The principal POCs π_{im} (with the indices i and m corresponding respectively to the light polarization direction and the mechanical stress component σ_m) have been measured using a Mach–Zehnder interferometer. A sample under uniaxial mechanical stress was inserted into one of its arms, a so-called sample arm.

The change $\delta\Delta_k$ in the optical path between the sample and reference arms is described by the following relation (see, e.g., Ref. [5]):

$$\delta\Delta_k = -\frac{1}{2} \pi_{im} \sigma_m d_k n_i^3 + S_{km} \sigma_m d_k (n_i - 1). \quad (1)$$

Here n_i denotes the refractive index of the material, d_k the sample thickness along the light propagation direction k , and S_{km} the elastic compliance coefficients that define Poisson strains along the direction k .

The $\delta\Delta_k$ value can be determined issuing from a well-known method of half-wave stresses [6]. According to this method, we measure the parameter $\delta\Delta_k = \lambda/2$ (with $\lambda = 632.8$ nm being the light wavelength) which is achieved under the operative stress $\sigma_{im}^0 = \sigma_{im} d_k$. Taking the above definitions into account, one can rewrite Eq. (1) as

$$\pi_{im} = -\frac{\lambda}{\sigma_{im}^0 n_i^3} + \frac{2S_{km}}{n_i^3} (n_i - 1). \quad (2)$$

Thus, the POCs π_{im} can be determined from the experimental data σ_{im}^0 . As an example, one can use the following experimental conditions to determine π_{33} : (i) $k = 1$, $i = 3$, $m = 3$ or (ii) $k = 2$, $i = 3$, $m = 3$. According to the conditions (i) and (ii), we rewrite Eq. (2) as

$$\pi_{33} = -\frac{\lambda}{\sigma_{33}^0 n_3^3} + \frac{2S_{13}}{n_3^3} (n_3 - 1) \quad (3)$$

and

$$\pi_{33} = -\frac{\lambda}{\sigma_{33}^0 n_3^3} + \frac{2S_{23}}{n_3^3} (n_3 - 1). \quad (4)$$

Eqs. (3) and (4) differ only by the elastic compliance components. In principle, the equality $S_{13} = S_{23}$ is valid for the isotropic materials, the crystals of cubic system and the optically uniaxial crystals. Nonetheless, these two relations for π_{33} are important since they facilitate measuring the POC π_{33} in two different experimental geometries. This is convenient for checking the data obtained experimentally. The alternative relations for the other principal POCs can be formulated in a similar manner. Finally, it is easy to prove that the relationships like Eqs. (3) and (4) are not the same for the π_{11} and π_{22} coefficients, since they contain unequal elastic compliances S_{12} and S_{13} .

3. Results and discussion

Table 1 displays the operative stresses σ_{im}^o obtained experimentally and the principal POCs calculated on their basis for the $\text{Pb}_5\text{Ge}_3\text{O}_{11}$ crystals. The refractive indices $n_o = n_1 = n_2 = 2.116$ and $n_e = n_3 = 2.151$ ($\lambda = 632.8$ nm) [7] have been used for calculating π_{im} , together with the elastic compliances $S_{12} = -6.4$ and $S_{13} = -2.2$ (in the units $10^{-12} \text{ m}^2/\text{N} = 1 \text{ B}$) [8]. Unfortunately, we cannot calculate exactly the errors for the POC, since the errors for the elastic stiffness coefficients have not been indicated in Ref. [8]. Following from our recent studies, we present in Table 1 only the error values estimated in the present work.

Table 1. Results of our interferometric experiments performed for the $\text{Pb}_5\text{Ge}_3\text{O}_{11}$ crystals.

Experiment #	Experimental conditions			σ_{im}^o , kgf/cm	π_{im} , B *
	<i>m</i>	<i>k</i>	<i>i</i>		
1	1	2	1	$\sigma_{11}^o = 19$	$\pi_{11} = 2.08 \pm 0.39$
2			3	$\sigma_{31}^o = 29$	$\pi_{31} = 0.76 \pm 0.27$
3	1	3	1	$\sigma_{11}^o = 24$	$\pi_{11} = 2.32 \pm 0.29$
4			2	$\sigma_{21}^o = 29$	$\pi_{21} = 1.83 \pm 0.24$
5	2	1	2	$\sigma_{22}^o = 19.5$	$\pi_{22} = 1.99 \pm 0.38$
6			3	$\sigma_{32}^o = 29$	$\pi_{32} = 0.76 \pm 0.27$
7	2	3	2	$\sigma_{22}^o = 25$	$\pi_{22} = 2.21 \pm 0.28$
8			1	$\sigma_{12}^o = 33$	$\pi_{12} = 1.55 \pm 0.21$
9	3	1	3	$\sigma_{33}^o = 21.5$	$\pi_{33} = 2.51 \pm 0.31$
10			2	$\sigma_{23}^o = 48$	$\pi_{23} = 0.90 \pm 0.15$
11	3	2	3	$\sigma_{33}^o = 20$	$\pi_{33} = 2.73 \pm 0.33$
12			1	$\sigma_{13}^o = 46$	$\pi_{13} = 0.96 \pm 0.16$

* Brewster is defined as $1 \text{ B} = 10^{-12} \text{ m}^2/\text{N}$

Taking the equality $\pi_{11} = \pi_{22}$ into account, one can see that the POC π_{11} has been determined basing on the measurements in four different geometries (see lines 1, 3, 5 and 7 in Table 1). Notice also that the errors in the lines 3 and 7 are much smaller than those appearing in the lines 1 and 5. Then the final π_{11} error has been calculated from the results presented in the lines 3 and 7. The other POCs have been determined from the measurements in two different geometries, since we have $\pi_{12} = \pi_{21}$, $\pi_{13} = \pi_{31}$ and $\pi_{23} = \pi_{32}$. Finally, the resultant POCs are presented in terms of their mean arithmetic values and mean arithmetic errors (see Table 2).

By their magnitude, the largest POCs (π_{11} , π_{12} and π_{33}) for lead germanate are comparable with the POCs of such known piezo-optic crystals as GaP (of which maximal POC is equal to 1.44 B [5]), CaWO_4 (1.86 B [4]), LiNbO_3 (2.06 B [9]), SiO_2 (3.11 B [10]) and $\beta\text{-BaB}_2\text{O}_4$ (3.7 B [11]).

Table 2. Principal POCs and elasto-optic coefficients found for the lead germanate crystals.

π_{im}, B	π_{11}	π_{12}	π_{32}	π_{31}	π_{33}
Present work	2.27±0.28	1.69±0.23	0.93±0.16	0.76±0.27	2.62±0.32
p_{in}	p_{11}	p_{12}	p_{32}	p_{31}	p_{33}
Present work	0.217±0.026	0.193±0.022	0.159±0.019	0.116±0.022	0.274±0.040
Ref. [13]	0.223	0.213	0.129	0.194	0.202

The elasto-optic coefficients have been calculated, using a well-known tensor formula $p_{in} = \pi_{im}C_{mn}$, with C_{mn} being the elastic module tensor. For the point group of symmetry 3 we have

$$\begin{aligned}
 p_{11} &= \pi_{11}C_{11} + \pi_{12}C_{12} + \pi_{13}C_{13} + \pi_{14}C_{14} + \pi_{15}C_{15}, & p_{13} &= (\pi_{11} + \pi_{12})C_{13} + \pi_{13}C_{33}, \\
 p_{12} &= \pi_{11}C_{12} + \pi_{12}C_{11} + \pi_{13}C_{13} - \pi_{14}C_{14} - \pi_{15}C_{15}, & p_{31} &= \pi_{31}(C_{11} + C_{12}) + \pi_{33}C_{13}, \\
 p_{33} &= 2\pi_{31}C_{13} + \pi_{33}C_{33}.
 \end{aligned} \quad (5)$$

The elastic modules have been taken from Ref. [8]: $C_{11} = 6.84$, $C_{12} = 2.68$, $C_{13} = 1.79$, $C_{33} = 9.43$, $C_{14} = 0.0$, $C_{15} = -0.12$ (all in the units of 10^{10} N/m^2). The POCs π_{14} and π_{15} needed for the calculations have been determined in the work [12]: $\pi_{14} = -(0.35 \pm 0.09) \text{ B}$ and $\pi_{15} \leq |0.09| \text{ B}$. Since these coefficients are rather small and the same holds true for the elastic modules C_{14} and C_{15} , one can neglect the fourth and fifth terms in the first and second lines of Eqs. (5). The elasto-optic coefficients calculated in this manner are presented in Table 2.

It is seen from Table 2 that the elasto-optic coefficients determined by us agree well with those measured in Ref. [14] using an AO-based Dixon–Cohen method. The only exceptions are the elasto-optic coefficients p_{31} and p_{33} , especially the largest p_{33} coefficient.

Now let us consider an isotropic AO Bragg diffraction inside the principal crystal-physical planes, under the conditions that quasi-longitudinal acoustic waves (AWs) interact with optical waves and the AWs propagate close to the principal coordinate axes. A schematic view of the appropriate wave-vector diagrams is given in Fig. 1. Note that a purely longitudinal AW propagates along the principal axis Z . The quasi-longitudinal AW propagating along the Y axis also becomes purely longitudinal since C_{14} is equal to zero [8]. Finally, a quasi-longitudinal AW propagating along the X axis is nearly longitudinal, with the angle of non-orthogonality of its polarization not exceeding ~ 1.5 deg. Hence, in our further analysis one can neglect the non-orthogonality of the longitudinal AWs that propagate along the principal directions.

The AO figure of merit for lead germanate (see Table 3) has been calculated using a standard relation $M_2 = n^6 p_{eff}^2 / \rho v^3$, where p_{eff} implies the effective elasto-optic coefficient, $\rho = 7330 \text{ kg/m}^3$ [8] the crystal density and v the velocity of the longitudinal AW. The latter has been taken from Ref. [14].

The highest AO figure of merit, $24.3 \times 10^{-15} \text{ s}^3/\text{kg}$, can be reached at the type I of AO interactions with the longitudinal AW propagating along the Z axis. Almost the same AO figure of merit, $21.2 \times 10^{-15} \text{ s}^3/\text{kg}$, is achieved for the interaction geometries given by Eqs. (3), (5) and (7). Note that, according to the maximal AO figure of merit, $\text{Pb}_5\text{Ge}_3\text{O}_{11}$ is comparable with β -barium borate [12] and lead molybdate crystals [14]. Moreover, the maximal figure of merit for the lead germanate crystals exceeds essentially the appropriate values for such known AO materials as, e.g., lithium niobate [15, 16], crystalline quartz and fused silica [15]. Nonetheless, the longitudinal AWs propagating along the principal crystal-physical axes manifest usually large enough

attenuations in the high-frequency range [14]. Then it would be necessary to decrease the operative acoustic frequency down to MHz range, if one needs to use the AO parameters of lead germanate mentioned above. On the other hand, one can consider the AO interactions in the other geometries, as well as the interactions with the other AWs. In the latter case, all of the elasto-optic tensor components need to be determined. These points will be a subject of our forthcoming works.

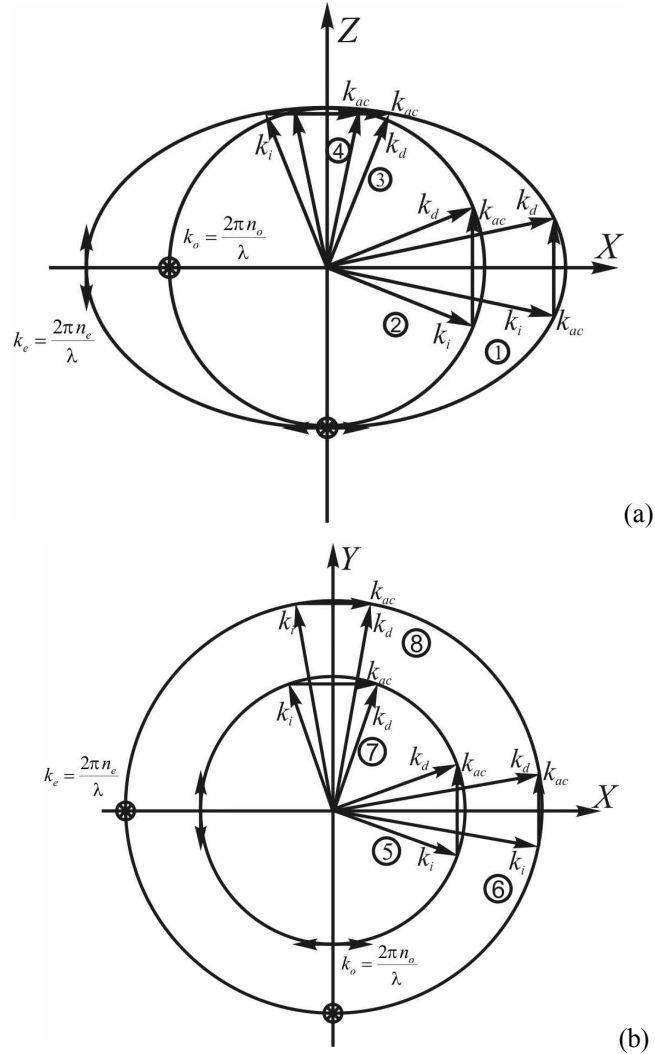


Fig. 1. Schematic wave-vector diagrams for XZ (a) and XY (b) planes: k_{ac} is the acoustic wave vector, while k_i and k_d are the wave vectors of the incident and diffracted optical waves, respectively. Double-sided arrows and crossed circles indicate polarizations of the optical waves.

Table 3. AO figure of merit calculated for the $Pb_5Ge_3O_{11}$ crystals.

Type of isotropic interaction	1	2	3	4	5	6	7	8
AW velocity, m/s	3470	3470	3010	3010	3010	3010	3010	3010
Refractive index	n_e	n_o	$n_e \approx n_o$	n_o	n_o	n_e	n_o	n_e
P_{eff}	P_{33}	P_{13}	P_{11}	P_{12}	P_{11}	P_{31}	P_{11}	P_{31}
AO figure of merit, $10^{-15} s^3/kg$	24.3	7.4	21.2	16.8	21.2	7.1	21.2	7.1

4. Conclusions

In the present work we have determined experimentally the principal POCs for the lead germanate crystals. On the basis of those results, the elasto-optic coefficients have been calculated and the AO figure of merit of $\text{Pb}_5\text{Ge}_3\text{O}_{11}$ has been estimated for the case of AO interactions with the longitudinal AWs propagating close to the principal crystal-physical directions. It has been found that the highest AO figure of merit, $24.3 \times 10^{-15} \text{ s}^3/\text{kg}$, is reached at the AO interaction with the longitudinal AW propagating along the Z axis. Almost the same AO figures of merit are peculiar for a number of different interaction geometries. As a result, the AO parameters of the $\text{Pb}_5\text{Ge}_3\text{O}_{11}$ crystals are comparable with the characteristics of many known AO materials. However, due to high attenuation typical in the GHz frequency range for the longitudinal AWs propagating along the principal crystal-physical axes, lead germanate must be used in some other geometries of AO interactions (e.g., the interactions with shear AWs) or in the lower-frequency range.

Acknowledgement

The authors acknowledge financial support of this study from the Ministry of Education and Science of Ukraine (the Project #0118U003899).

References

1. Iwasaki H, Miyazawa S, Koizumi H, Sugii K and Niizeki N, 1972. Ferroelectric and optical properties of $\text{Pb}_5\text{Ge}_3\text{O}_{11}$ and its isomorphous compound $\text{Pb}_5\text{Ge}_2\text{SiO}_{11}$. *J. Appl. Phys.* **43**: 4907–4915.
2. Sirotin Y I and Shaskolskaya M P. *Fundamentals of crystal physics*. Moscow: Mir (1982).
3. Mytsyk B, Demyanyshyn N, Erba A, Shut V, Mozzharov S, Kost Ya, Mys O and Vlokh R, 2017. Piezo-optic and elasto-optic properties of monoclinic triglycine sulfate crystals. *Appl. Opt.* **56**: 9484–9490.
4. Mytsyk B G, Kost' Ya P, Demyanyshyn N M, Gaba V M and Sakharuk O M, 2015. Study of piezo-optic effect of calcium tungstate crystals by the conoscopic method. *Opt. Mater.* **39**: 69–73.
5. Mytsyk B G, Andrushchak A S and Kost' Ya P, 2012. Static photoelasticity of gallium phosphide crystals. *Crystallogr. Rep.* **57**: 124–130.
6. Sonin A S and Vasilevskaya A S. *Electro-optic crystals*. Moscow: Atomizdat (1971).
7. Iwasaki H and Sugii K, 1971. Optical activity of ferroelectric $5\text{PbO} \cdot 3\text{GeO}_2$ single crystals. *Appl. Phys. Lett.* **19**: 92–93.
8. Yamada T, Iwasaki H and Niizeki N, 1972. Elastic and piezoelectric properties of ferroelectric $5\text{PbO} \cdot 3\text{GeO}_2$ crystals. *J. Appl. Phys.* **43**: 771–775.
9. Krupych O, Savaryn V and Vlokh R, 2014. Precise determination of full matrix of piezo-optic coefficients with a four-point bending technique: the example of lithium niobate crystals. *Appl. Opt.* **53**: B1–B7.
10. Narasimhamurthy T S, 1969. Photoelastic constants of α -quartz. *J. Opt. Soc. Amer.* **59**: 682–686.
11. Andrushchak A S, Bobitski Y V, Kaidan M V, Tybinka B V, Kityk A V and Schranz W, 2004. Spatial anisotropy of photoelastic and acoustooptic properties in β - BaB_2O_4 crystals. *Opt. Mater.* **27**: 619–624.
12. Vasylyk Yu, Skab I and Vlokh R, 2011. Measurements of piezo-optic coefficients π_{14} and π_{25} in $\text{Pb}_5\text{Ge}_3\text{O}_{11}$ crystals using torsion induced optical vortex. *Ukr. J. Phys. Opt.* **12**: 101–108.
13. Ohmachi Y and Uchida N, 1972. Acoustooptic property of single-crystal $5\text{PbO} \cdot 3\text{GeO}_2$. *J. Appl. Phys.* **43**: 3583–3584.

14. Shaskolskaya M P. Acoustic crystals. Moscow: Nauka (1982).
15. Mys O, Kostyrko M, Krupych O and Vlokh R, 2015. Anisotropy of the acousto-optic figure of merit for LiNbO₃ crystals: isotropic diffraction. Appl.Opt. **54**: 8176–8186.
16. Mys O, Kostyrko M and Vlokh R, 2016. Anisotropy of acousto-optic figure of merit for LiNbO₃ crystals: anisotropic diffraction. Appl.Opt. **55**: 2439–2450.

Mytsyk B., Demyanyshyn N., Adamenko D., Trubitsyn M. and Vlokh R. 2019. Principal components of piezo-optic tensor for Pb₅Ge₃O₁₁ crystals. Ukr.J.Phys.Opt. **20**: 91 – 97.
doi: 10.3116/16091833/20/3/91/2019

***Анотація.** З використанням інтерферометричної методики і методу пів-хвильових напружень в роботі визначені головні компоненти п'єзооптичного тензора π_{im} (π_{11} , π_{12} , π_{13} , π_{31} , π_{33}) кристалів германату свинцю. На основі експериментально отриманих п'єзооптичних коефіцієнтів розраховані відповідні коефіцієнти пружно-оптичного тензора p_{im} , а також оцінені значення коефіцієнтів акусто-оптичної якості. Виявлено, що максимальне значення $M_2=24.3 \times 10^{-15} \text{ c}^3/\text{кг}$, для кристалів Pb₅Ge₃O₁₁ є співмірним з відповідними коефіцієнтами кристалів β -борату барію і молібдату свинцю. Крім того, це значення для германату свинцю значно перевищує відповідні коефіцієнти для таких відомих акустооптичних матеріалів, як ніобат літію і кристалічний та плавлений кварц.*